J. Cell. Mol. Med. Vol 16, No 6, 2012 pp. 1298-1309

A new oncolytic adenoviral vector carrying dual tumour suppressor genes shows potent anti-tumour effect

Xin-Ran Liu [a, b, #], Ying Cai [a, #], Xin Cao [a], Rui-Cheng Wei [a], Hui-Ling Li [a], Xiu-Mei Zhou [c], Kang-Jian Zhang [a], Shuai Wu [a], Qi-Jun Qian [c, d], Biao Cheng [b], Kun Huang [b, *], Xin-Yuan Liu [a, c, *]

[a] *Laboratory of Molecular Cell Biology, Institute of Biochemistry and Cell Biology, Shanghai Institutes for Biological Sciences, Chinese Academy of Sciences, Shanghai, China*
[b] *TongJi School of Pharmacy, Huazhong University of Science & Technology, Wuhan, China*
[c] *Xinyuan Institute of Medicine and Biotechnology, Zhejiang Sci-Tech University, Hangzhou, China*
[d] *Eastern Heptobiliary Hospital, Second Military Medical University, Shanghai, China*

Received: May 17, 2011; Accepted: July 22, 2011

Abstract

Cancer Targeting Gene-Viro-Therapy (CTGVT) is a promising cancer therapeutical strategy that strengthens the anti-tumour effect of oncolytic virus by expressing inserted foreign anti-tumour genes. In this work, we constructed a novel adenoviral vector controlled by the tumour-specific survivin promoter on the basis of the ZD55 vector, which is an E1B55KD gene deleted vector we previously constructed. Compared with the original ZD55 vector, this new adenoviral vector (ZD55SP/E1A) showed much better ability of replication and reporter gene expression. We then combined anti-tumour gene interleukine-24 (IL-24) with an RNA polymerase III-dependent U6 promoter driving short hairpin RNA (shRNA) that targets M-phase phosphoprotein 1 (MPHOSPH1, a newly identified oncogene) by inserting the IL-24 and the shRNA of MPHOSPH1 (shMPP1) expression cassettes into the new ZD55SP/E1A vector. Our results demonstrated excellent anti-tumour effect of ZD55SP/E1A-IL-24-shMPP1 *in vitro* on multiple cancer cell lines such as lung cancer, liver cancer and ovarian caner. At high multiplicity-of-infection (MOI), ZD55SP/E1A-IL-24-shMPP1 triggered post-mitotic apoptosis in cancer cells by inducing prolonged mitotic arrest; while at low MOI, senescence was induced. More importantly, ZD55SP/E1A-IL-24-shMPP1 also showed excellent anti-tumour effects *in vivo* on SW620 xenograft nude mice. In conclusion, our strategy of constructing an IL-24 and shMPP1 dual gene expressing oncolytic adenoviral vector, which is regulated by the survivin promoter and E1B55KD deletion, could be a promising method of cancer gene therapy.

Keywords: MPHOSPH1 • oncolytic adenoviral vector • mitotic arrest • post-mitotic apoptosis • cancer gene therapy

Introduction

Current anti-mitotic drugs for cancer, including vinca alkaloids and taxanes, function by disturbing spindle assembly, which activates the spindle assembly checkpoint (SAC) and causes mitotic arrest and triggers apoptosis [1]. However, all these drugs also exhibit side effects, including neurotoxicity, presumably due to the perturbation of microtubules in neurons [2]. As an effort to develop new anti-mitotic targets without this defect, in this study, we focused on a novel combination of IL-24 and MPHOSPH1, a newly discovered oncogene. MPHOSPH1 is a member of the kinesin superfamily. It is a plus-end-directed molecular motor playing important roles in cytokinesis [3]. Kanehira *et al.* recently found that MPHOSPH1 was up-regulated in bladder cancer, and MPHOSPH1 knockdown resulted in cytokinesis defect that significantly inhibited the growth of bladder cancer cells [4], which made it a potential target for cancer gene therapy. In this study, we found for the first time that in addition to previously reported bladder cancer cells, MPHOSPH1 was also up-regulated in multiple cancer cells. MPHOSPH1 knockdown caused mitotic arrest without activation

[#]These authors contributed equally to this work.
*Correspondence to: Xin-Yuan LIU,
320 Yue Yang Road, Shanghai 200031, China.
Tel.: +86 21 54921126
Fax: +86 21 54921126
E-mail: xyliu@sibs.ac.cn

Kun HUANG,
13 Hang Kong Road,
Wuhan 430030, China.
Tel.: +86 27 83691499
Fax: +86 27 83691499
E-mail: kunhuang2008@hotmail.com

doi:10.1111/j.1582-4934.2011.01396.x

of SAC, which may be attributed to a lack of effect on microtubules (spindle), followed by post-mitotic apoptosis.

Another promising anti-oncogene on which we focused in this work was IL-24, which has been proven as a safe and potent tumour suppressor gene, and has been widely used in cancer gene therapy [5, 6]. It has been reported that the anti-tumour effects of IL-24 include apoptosis, endoplasmic reticulum stress, autophagy and radiosensitizing of tumour cells [7–15].

In 2001, we designed a cancer treating strategy called CTGVT, which combines gene therapy with oncolytic viral therapy by inserting an anti-tumour gene into the oncolytic viral vector [16]. Our previous CTGVT work used the ZD55 vector, which was based on the deletion of E1B55KD gene, as the oncolytic adenoviral vector (OV) [17]. Deletion of adenoviral E1B55KD, an adenovirus early gene, resulted in the loss of replication capacity of adenovirus (Ad) in normal cells but not in tumour cells, and thus confer new tumour-specific replication property to adenovirus [18]. Similar E1B55KD gene deletion strategy has also been used in ONYX-015, the first generation of commercial oncolytical virus product [19]. We have also demonstrated that the ZD55-gene system could be a potent anti-tumour strategy [5, 17, 20, 21]. Despite its successful applications, disadvantages of this adenovirus have also been reported. For example, we observed impaired replication ability and even certain liver toxicity of ZD55 vector [17, 22]. To improve the replication ability of the ZD55 vector in tumour tissue and its safety in normal tissue, in this study, we replaced its E1A promoter with a 269 bp tumour-specific survivin promoter, and named this new vector ZD55SP/E1A. The replication of this new vector is controlled by two mechanisms (both genetic deletion of E1B55KD and survivin promoter-controlled E1A). We then used this dual regulated vector ZD55SP/E1A to express tumour suppressor gene IL-24 and shRNAs targeting MPHOSPH1 (shMPP1) in cancer cells. Our results showed that ZD55SP/E1A-IL-24-shMPP1 had excellent anti-tumour effects both *in vitro* and *in vivo*. We also found that cIAP down-regulation may contribute to the enhanced anti-tumour effects of ZD55SP/E1A-IL-24-shMPP1. Taken together, our results suggested that ZD55SP/E1A-IL-24-shMPP1 could be a highly promising agent for cancer gene therapy.

Materials and methods

Cell lines and culture conditions

Detailed information for cell lines used in this study and their culturing conditions can be found in the Supporting Material.

Construction of the adenoviral plasmids

The adenoviral packaging plasmid pBHGE3 was obtained from Microbix Biosystems (Toronto, Ontario, Canada). The adenoviral shuttle plasmids pZXC2, pZDΔ55 and pCA13-IL-24 were constructed as we previously described [5, 17, 23]. Detailed information on the construction of adenoviral plasmids can be found in the Supporting Material.

Luciferase assay

pGL3-Basic (promoter-free) and pGL3-Control (SV40 promoter) were used as the luciferase reporter plasmids. The survivin promoter on pTG19-SP was cloned into pGL3-Basic to generate the luciferase reporter plasmid pGL3-SP. One day before transfection, $0.5–2\times10^5$ cells were seeded in 24-well plates. The cells were transfected with pGL3-SP by Lipofectamine2000 (Invitrogen, Carlsbad, CA, USA) and also with pGL3-Basic and pGL3-Control as controls. The cells were harvested 48 hrs later, and the luciferase activity was assayed by the dual-luciferase reporter assay system (Promega, Madison, WI, USA).

Generation, identification, production, purification and titration of the oncolytic adenovirus

The recombinant adenovirueses (rec-Ads) (ZD55SP/E1A, ZD55SP/E1A-IL-24, ZD55SP/E1A-shMPP1, ZD55SP/E1A-IL-24-shMPP1 and ZD55SP/E1A-EGFP) were generated by respective homologous recombination between the transfer plasmids (pSP-Δ55, pSP-IL-24-Δ55, pSP-shMPP1-Δ55, pSP-IL-24-shMPP1-Δ55 and pSP-EGFP-Δ55) and packaging plasmid pBHGE3 in HEK293 cells. The detailed procedures for generation, identification, production, purification and titration of the recombinant adenovirus are provided in the Supporting Material.

RT-PCR analysis

Total RNA was isolated from cells using Trizol (Invitrogen). A total of 2 μg of RNA was used to synthesize the first single-strand cDNA for PCR amplification using RevertAid™ First Strand cDNA Synthesis Kit (Fermentas, Vilnius, Lithuania). The relative quantification of MPHOSPH1 cDNA and adenovirus gene E3 cDNA was measured by using the ABI 7500 Fast System and the Bio-Rad CFX96™ Real-Time PCR Detection System with Power SYBR® Green PCR Master Mix (Applied Biosystems, Carlsbad, CA, USA), with GAPDH cDNA as an internal standard, with primers as follows:

Forward: 5′-AGA AAC CAA CAG GCA AGA AAC-3′
Reverse: 5′-CTC ATC ACG CAT TAC AGA TAC C-3′
Forward: 5′-AAC AGA GAT GAC CAA CAC AAC-3′
Reverse: 5′-CAG ATG AGC CAC ATA ATA ATA AGG-3′
Forward: 5′-GGT GAA GGT CGG AGT CAA CGG A-3′
Reverse: 5′-GAG GGA TCT CGC TCC TGG AAG A-3′

Cytotoxicity assay

Tumour cells and normal cells were seeded in 24-well plates, and 24 hrs later, they were infected with Ads at various MOIs. Four days after infection, the medium was removed, and the cells were exposed to 2% crystal violet in 20% methanol for 20 min. The plates were then washed with water and documented as photographs.

Cell viability assay

SW620 and BEL-7404 were seeded in 96-well plates, and 24 hrs later, they were infected with Ads at MOI of 1. At 24, 48, 72 and 96 hrs after the infection, 20 ml of 3-(4,5-dimethylthiazol-2-yl)-2,5-diphenyltetrazolium bromide (MTT; 5 mg/ml) was added to each well, and the plates were incubated at 37°C for four hrs. The medium was then removed and 100 ml of 0.04M HCl–isopropanol solution was added to each well. Absorbance at 595 and 655 nm was measured using a Microplate Reader (Thermo, Asheville, NC, USA). Ten replicate wells were counted for each assay.

Cell nuclei and skeleton staining assay

Cells were seeded on glass cover slips in six-well plates, and 24 hrs later they were infected with Ads at MOI of 1. Cells were then fixed with 0.5 ml of 4% paraformaldehyde for 10 min., washed twice with PBS, stained with Phalloidin Alexa Fluor 555 (Molecular Probes, Eugene, OR, USA), washed twice with PBS, stained with DAPI (Sigma-Aldrich, St. Louis, MO, USA) or Hoechst 33258 (Molecular Probes), and washed twice with PBS. Cells were observed using a BX51 upright microscope (Olympus, Tokyo, Japan) or a Leica TCS SP2 confocal microscope (Leica Microsystems, Wetzlar, Germany).

Western blot assay

Cells were harvested and washed with PBS, and then lysed in SDS-PAGE sample buffer. Protein concentrations were determined using the Bio-Rad protein assay buffer. A total of 50 μg of protein was separated on 8–15% polyacrylamide gels and transferred to Polyvinylidene Fluoride (PVDF) membranes (Millipore, Billerica, MA, USA). Detailed information for the antibodies used in this study can be found in the Supporting Material.

Flow cytometric analysis

For propidium iodide (PI) staining, cells were harvested and washed with PBS, fixed with 70% ethanol at 4°C for 30 min. The cells were then washed with PBS and incubated at 37°C for 30 min. with RNase A, washed with PBS and stained with PI (50 μg/ml) for 30 min. to be ready for fluorescence-activated cell sorting (FACS) analysis. For JC-1 staining, cells were harvested and resuspended in 0.5 ml of medium, and 0.5 ml of 5 μg/ml JC-1 fluorescent probe (Sigma-Aldrich) was added into the medium; the cells were incubated at 37°C for 20 min. and washed with PBS and were ready for FACS analysis. For fluorescein isothiocyanate (FITC) and PI double-staining FACS, an Annexin V-FITC Kit (Bender MedSystems, Vienna, Austria) was used, and the cells were treated according to the manufacturer's instructions. The FACS assay was performed on a FACSCalibur flow cytometer (BD Biosciences, Franklin Lakes, NJ, USA) immediately after staining.

SA-β-gal staining assay

β-Galactosidase staining was performed with a senescence-associated β-Galactosidase Staining Kit (Beyotime, Shanghai, China). Cells were washed three times with PBS and fixed with 4% paraformaldehyde for 15 min. at room temperature. Next, the cells were incubated overnight at 37°C in darkness with the working solution containing 0.05 mg/ml X-gal.

Animal experiments

Animal experiments were performed according to the SIBS Guideline for the Care and Use of Laboratory Animals. Male BALB/c nude mice (4-week old) were purchased from the Shanghai Experimental Animal Center (Shanghai, China). To establish xenograft tumours, 5×10^6 SW620 cells in 150 μl DMEM were subcutaneously injected into the right flank of each mouse. When tumours reached 100–150 mm^3 in volume, mice were divided randomly into five groups (seven mice per group). A total of 2×10^9 PFUs of Ads per mouse or PBS were injected every other day into the tumours for four times. Tumour volume (mm^3) was measured by a Vernier calliper every week and calculated by length (mm) × width (mm) × width (mm)/2.

Immunohistochemistry and terminal deoxynucleotidyl transferase-mediated dUTP biotin nick end-labelling assay

Tumour tissues were fixed in 4% formaldehyde for 2 days, dehydrated in 30% sucrose solution and embedded in Jung tissue freezing medium (Leica Microsystems, Nussloch Gmbh, Nussloch, Germany) at −80°C. Detailed procedures of immunohistochemistry and terminal deoxynucleotidyl transferase-mediated dUTP biotin nick end labelling (TUNEL) assay can be found in the Supporting Material.

Statistical analysis

All data were expressed as the mean ± S.D. and were analysed using independent sample *t*-tests and one-way ANOVA using SPSS Base 10.0. Results were considered statistically significant when $P < 0.05$.

Results

Clone of survivin promoter and its tumour-specific transcriptional activity

Survivin is a member of the inhibitor of apoptosis (IAP) family. We had previously took advantage of survivin differential expression in tumour tissues *versus* normal tissues [24–26], to construct oncolytic adenovirus with a 1.1 kb survivin promoter [27]. In this study, a further shortened 269 bp survivin promoter was used to construct a luciferase reporter plasmid containing this short promoter. Promoter activity was determined by the luciferase activity after transient transfection. In SW620 and HeLa cells, the luciferase expression level driven by the short survivin promoter was similar to that driven by the strong SV40 viral promoter (pGL3-Control), and was much higher than that observed with the

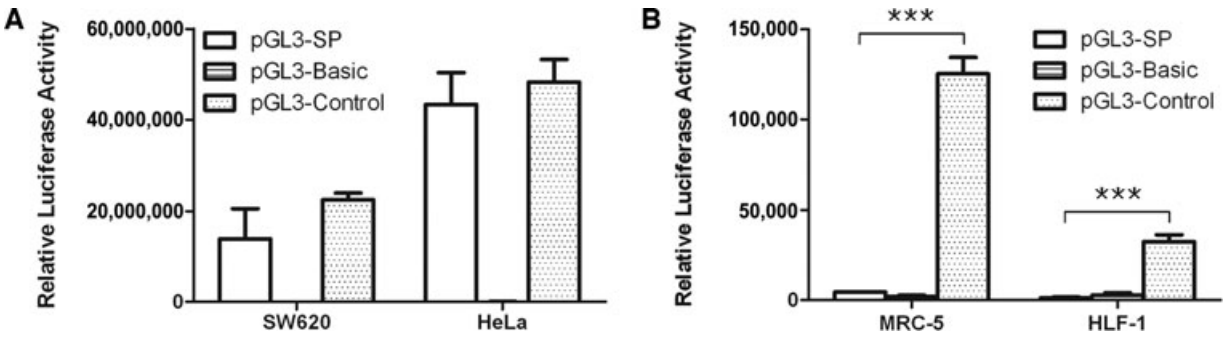

Fig. 1 Transcriptional activity of the 269 bp survivin promoter. The relative activities of the survivin promoter in tumour cells SW620 and HeLa (**A**) or in normal cells MRC-5 and HLF-1 (**B**) were measured by the luciferase assay system. Data are presented as mean ± S.D. (bars) ($n = 4$, $***P < 0.001$). A total of 0.7 μg of reporter plasmid together with 0.07 μg of pCMV-β-gal were co-transfected. Forty-eight hours later, the cells were harvested, and the luciferase activity was assayed by the dual-luciferase reporter assay system.

promoterless control (Fig. 1A). In contrast, in transient transfected normal MRC-5 and HLF-1 cells, only baseline levels of luciferase expression were observed (Fig. 1B). All these results suggested that the short 269 bp survivin promoter has a strict tumour-selective transcriptional activity.

MPHOSPH1 is up-regulated in various tumour cells

It has been reported that MPHOSPH1 is up-regulated in bladder cancer cells but not in normal human tissues [4]. To evaluate MPHOSPH1 levels in different cancer cells, we employed quantitative real-time PCR to analyse the levels of MPHOSPH1 mRNA. We found that MPHOSPH1 was up-regulated not only in the bladder cancer cells (SCaBER and T24 cells), but also in many other types of cancer (HeLa, A549, BEL-7404 and SW620 cells); whereas it remained at low levels in normal cells (MRC-5 and L-02 cells; Fig. 2), which suggested MPHOSPH1 may be an ideal target in cancer gene therapy.

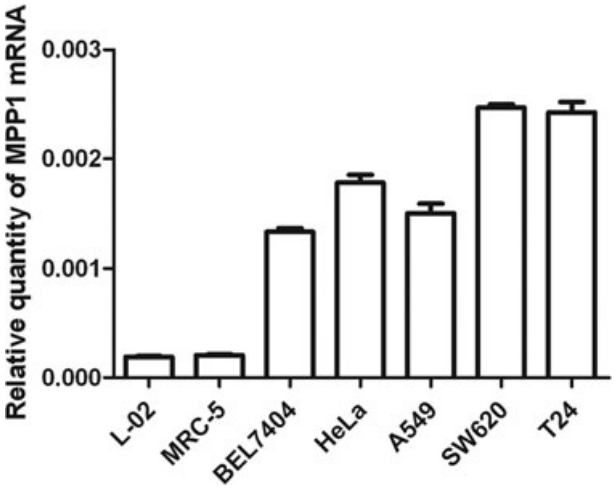

Fig. 2 Quantification of the MPHOSPH1 transcript level in various cell lines. The relative levels of MPHOSPH1 mRNA in five tumour and two normal cell lines were examined by RT-PCR. GAPDH was used as an internal control. Data are presented as mean ± S.D. (bars) ($n = 3$).

The new OV ZD55SP/E1A showed better replication ability and higher foreign gene delivery efficiency than ZD55

The OV ZD55SP/E1A is constructed based on the ZD55 vector [17]. In this study, the E1A promoter in the original wild-type serotype 5 Ad was replaced by the short 269 bp survivin promoter, and the E1B55KD was also deleted. Expression cassettes of both IL-24 and shMPP1 were then inserted into this new vector (Fig. 3A).

We measured the relative replicating multiples of both oncolytic Ads ZD55SP/E1A and ZD55 by RT-PCR using the adenovirus gene E3 cDNA. Our result suggested that ZD55SP/E1A had a better replication ability than that of the ZD55 in tumour cells SW620 and HeLa, while in normal MRC-5 cells, both Ads showed low replication abilities (Fig. 3B). We also assessed the gene-expression ability of this new OV, the result is consistent with our replication assay results (Fig. 3B–E). ZD55SP/E1A-EGFP, an oncolytic adenovirus carrying EGFP reporter gene, showed much stronger fluorescence than ZD55-EGFP after infecting A549 and SW620 cells for 96 hrs, while very weak fluorescence was observed in infected normal MRC-5 cells (Fig. 3C–E). All these results suggested that compared with the ZD55 vector, the OV ZD55SP/E1A has comparable safety in normal cells, and much better replication ability and higher extraneous gene delivery efficiency in tumour cells.

We subsequently inserted both the IL-24 and shMPP1 expression cassettes into the ZD55SP/E1A OV, and the results on the identification of rec-Ads are provided in the Supporting Material.

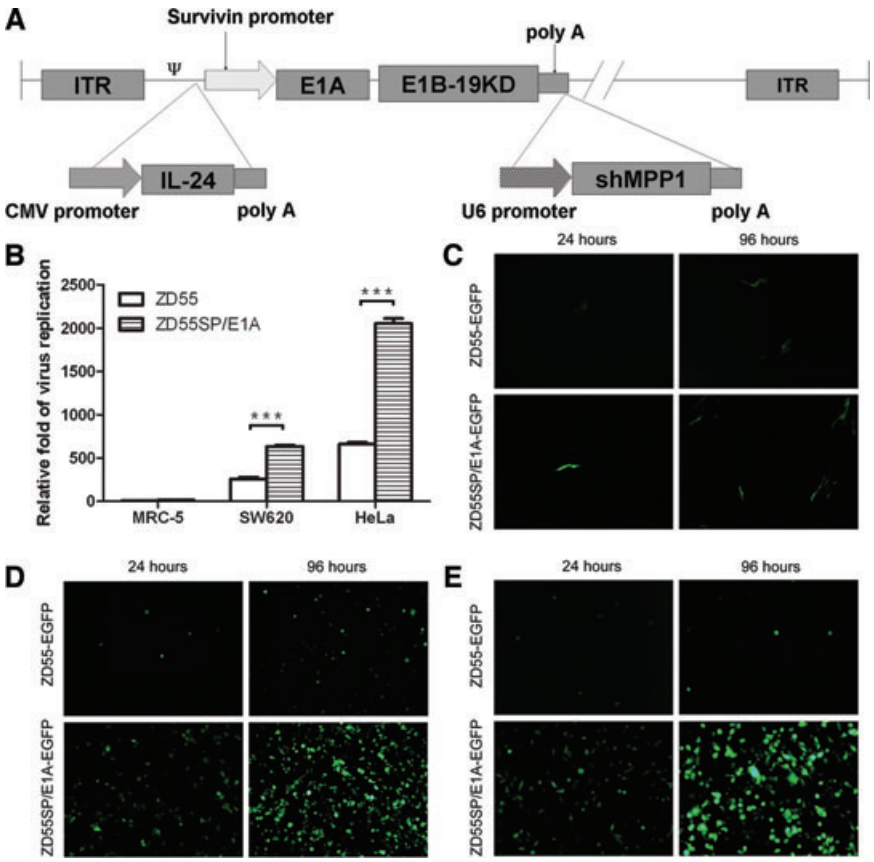

Fig. 3 Characterization of the OV ZD55SP/E1A. (**A**) A schematic drawing of the oncolytic Ad ZD55SP/E1A-IL-24-shMPP1. Ψ is the encapsidation signal; ITR is the inverted terminal repeat. (**B**) Analysis of the replication ability of ZD55SP/E1A and ZD55 in the normal (MRC-5) and tumour cells (SW620 and HeLa) by RT-PCR. The adenovirus E3 region was amplified to evaluate the viral DNA content at 48 hrs after infection (MOI = 0.1). Data are presented as mean ± S.D. (bars) ($n = 3$, $^{***}P < 0.001$). (**C**–**E**) EGFP as a reporter gene. Normal-MRC-5 (**C**) and tumour cells A549 (**D**) or SW620 cells (**E**) were infected with ZD55SP/E1A-EGFP and ZD55-EGFP at an MOI of 0.2. EGFP expression was assessed by photomicrographic examination at 24 and 96 hrs after infection.

For two Ads expressing the individual genes and the dual expressing construct, similar levels of IL-24 expression and inhibition of MPP1 were identified (Fig. S2C and D).

ZD55SP/E1A-IL-24-shMPP1 specifically inhibits tumour cell proliferation

MPHOSPH1 has been reported as a potential oncogene, and knockdown of MPHOSPH1 suppressed the growth of bladder cancer cells [4]. Here, to evaluate the anti-tumour ability of the OV expressing shMPP1 *in vitro*, we measured the cytopathic effect and cell viability by crystal violet staining and MTT assay. We found that besides the bladder cancer cells (SCaBER, data not shown), a number of other cancer cells (SW620, A549 and BEL-7404) were also sensitive to ZD55SP/E1A-IL-24-shMPP1 infection, whereas the normal MRC-5 and BEAS-2B cells showed much lower sensitivity (Fig. 4A), demonstrating the safety of ZD55SP/E1A-IL-24-shMPP1 in normal cells.

Further MTT results revealed the oncolytic effect of different adenoviruses in details. As shown in Figure 4B, from day 3, a visible decrease of cell viability was observed in all of the oncolytic Ads treating groups compared with the control group; on day 4, the decrease was 17.1% in BEL-7404 cells and 38.8% in SW620 cells treated with ZD55SP/E1A, while the decrease was 64.9% in BEL-7404 cells and 82.4% in SW620 cells treated with ZD55SP/E1A-IL-24-shMPP1 ($P < 0.001$), suggesting ZD55SP/E1A-IL-24-shMPP1 has the highest anti-tumour activity among the four rec-Ads we constructed.

ZD55SP/E1A-IL-24-shMPP1 induces polyploidy and apoptosis in SW620

One morphological change induced by ZD55SP/E1A-IL-24-shMPP1 during the early stage after infection was the increase in the number of multinuclear cells. As the FACS results suggested, the ZD55SP/E1A-IL-24-shMPP1 treatment significantly increased the number of the SW620 cells with >4N DNA content after 24 hrs (Fig. 5A). Visualization using confocol laser scanning microscopy (CLSM) also confirmed an accumulation of multinuclear cells 24 hrs after infection (Fig. 5B). Moreover, the multinuclear SW620 cells treated with ZD55SP/E1A-IL-24-shMPP1 began to show apoptosis at 36 hrs after infection (Fig. 5C).

To validate that the cell death induced by the Ads was apoptosis mediated, we infected SW620 cells with various rec-Ads, and

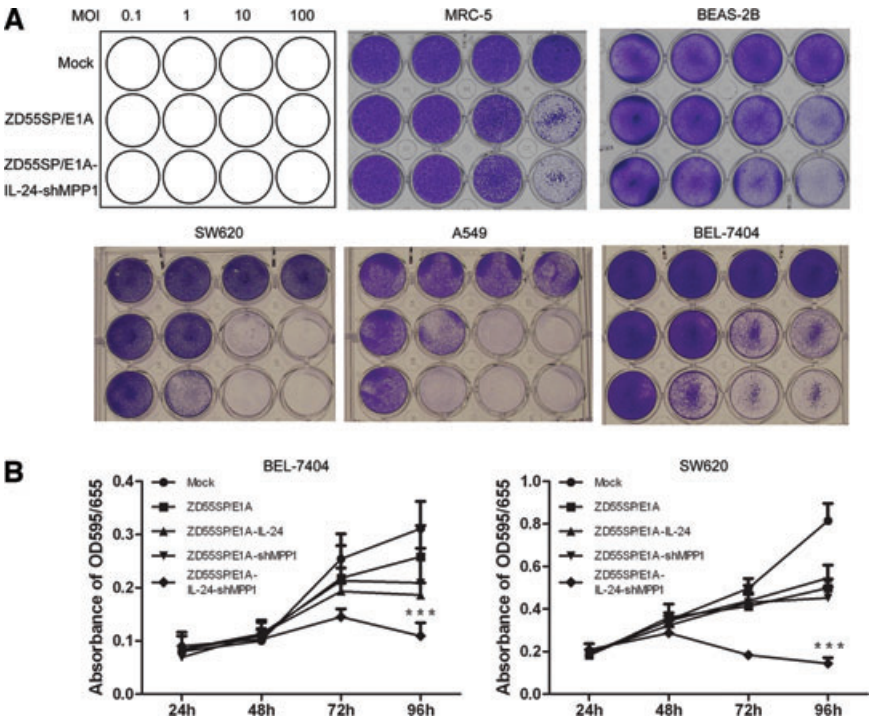

Fig. 4 ZD55SP/E1A-IL-24-shMPP1 specifically inhibited the growth of tumour cells. (**A**) The cytopathic effects of different rec-Ads on SW620, A549, BEL-7404, MRC-5 and BEAS-2B cells at varied MOIs were studied by crystal violet staining 96 hrs after infection. (**B**) Measurement of cell viability of BEL-7404 cells (left) and SW620 cells (right) every 24 hrs after infection with different Ads at MOI of 1 by MTT assay. Points indicate the mean values ($n = 10$); bars indicate S.D. ($***P < 0.001$).

48 hrs later, nuclear fragmentation and chromatin condensation was found in the rec-Ads-treated cells (Fig. 5D). FACS analysis was also performed 48 hrs after infection; SW620 cells were stained with annexin V-FITC and PI and evaluated for apoptosis. As shown in Figure 5E, the proportion of annexin V-positive SW620 cells infected with ZD55SP/E1A-IL-24-shMPP1 was 24.53%, much higher than the control (3.22%). We then applied JC-1 staining to examine the mitochondrial transmembrane electrical potential ($\Delta\Psi_m$) of SW620 cells by FACS. We found that 72 hrs after ZD55SP/E1A-IL-24-shMPP1 infection, 35.49% of the cells were detected with altered $\Delta\Psi_m$ (Fig. 5E). Therefore, we believed that ZD55SP/E1A-IL-24-shMPP1 may induce apoptosis *via* a mitochondria-dependent signalling pathway.

We further studied the levels of apoptosis-associated proteins after ZD55SP/E1A-IL-24-shMPP1 infection using Western blotting. As shown in Figure 5F, the cleavage products of Caspase-8, Caspase-9, Caspase-3 and PARP could be detected 48 hrs after ZD55SP/E1A-IL-24-shMPP1 infection, and by the time of 72 hrs, the cleavage products were enhanced, suggesting ZD55SP/E1A-IL-24-shMPP1 induces Caspase-8- and Caspase-9–mediated apoptosis. Another interesting result was that although all the rec-Ads can induce expression of cIAP, which can efficiently block TNF-mediated apoptosis [28, 29], only ZD55SP/E1A-IL-24-shMPP1 infection significantly inhibited cIAP expression 72 hrs after infection (Fig. 5F). Thus, the suppression of the cIAP may be the underlying mechanism by which the combination of IL-24 and shMPP1 shows strong synergistic anti-tumour effects.

ZD55SP/E1A-IL-24-shMPP1 induces mitotic arrest and senescence

To further clarify the relationship between polyploid status and apoptosis induced by the rec-Ads, A549 cells were infected with ZD55SP/E1A-IL-24-shMPP1 at MOI of 5, and 48 hrs later, we observed a remarkable accumulation of cells with >4N DNA content by FACS. However, the sub-G_1 peak was not distinct at 48 hrs, whereas 24 hrs later, the sub-G_1 peak markedly increased from 1.53% to 26.04% with the peak of >4N visually decreased (Fig. 6A). This observation suggested that most of the polyploid cells induced by ZD55SP/E1A-IL-24-shMPP1 were undergoing apoptosis. We then used phase-contrast videomicroscopy to examine the behaviour of the A549 cells infected with ZD55SP/E1A-IL-24-shMPP1 at MOI of 5 over a 72-hr duration. Approximately 36 hrs after infection, we observed a high proportion of multinuclear cells, and during the subsequent 24 hrs, many multinuclear cells were observed to be in a prolonged M phase. And with the time passing, a large number of cells in mitotic arrest underwent apoptosis (Fig. 6B).

Since p53 is often associated with post-mitotic apoptosis in cancer cells [30], we performed Western blot to investigate p53 and its downstream target genes of infected A549 cells, in which p53 was reported as wild type without any mutation [31]. As shown in Figure 6C, p53 was detected 24 hrs after infection, and enhanced expression of BTG2, Puma and Bax were observed as well. This result suggested that ZD55SP/E1A-IL-24-shMPP1 induced apoptosis after mitotic arrest through a p53 signalling

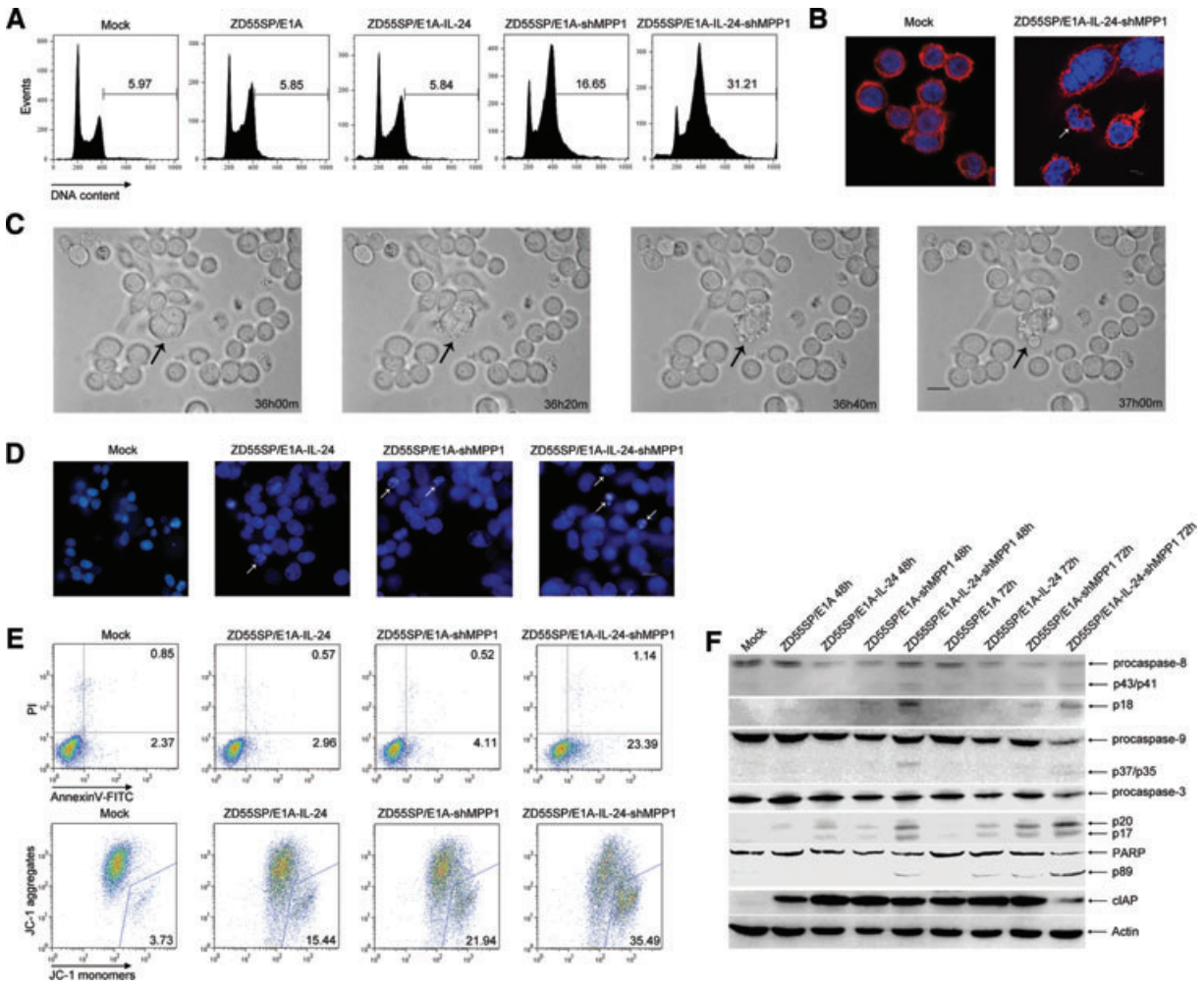

Fig. 5 ZD55SP/E1A-IL-24-shMPP1 induced apoptosis and polyploidy in tumour cells. (**A**) Analysis of the polyploid SW620 cells with PI staining by FACS 24 hrs after infection. The numbers show the percentage of cells with >4N DNA content. (**B**) Twenty-four hours after infection, the multinuclear SW620 cells stained with DAPI and Phalloidin Alexa Fluor 555 were visualized by confocal microscopy. The arrows point toward the multinuclear cells. Scale bar: 10 μm. (**C**) SW620 cells infected with ZD55SP/E1A-IL-24-shMPP1 were observed with multinuclear followed with apoptosis. Selected frames of the time lapse phase-contrast microscopy videos are shown. The arrow indicates the cell observed. Time is shown in hours and minutes. Scale bar: 20 μm. (**D**) The nuclear morphologies of SW620 cells stained with Hoechst33258 dye were visualized 48 hrs after infection. The arrows indicate the apoptotic cells. Scale bar: 20 μm. (**E**) The upper row, detection of apoptosis in SW620 cells using FACS with Annexin V-FITC and PI staining 48 hrs after infection. Numbers show the percentage of cells in the first and fourth quadrants; the lower row, analysis of the mitochondrial membrane potential of SW620 cells by FACS with JC-1 staining at 72 hrs after the infection. The percentage of cells in the trapeziform region is shown. (**F**) Western blot analysis of apoptosis-related proteins in SW620 cells infected with different Ads at 48 and 72 hrs after infection. p43/p41 and p18 are the cleaved products of procaspase-8. p37/p35 are the cleaved products of procaspase-9. p20 and p17 are the cleaved products of procaspase-3. p89 is a fragment of PARP. Actin was used as a loading control. (**A**–**F**) MOI = 1.

pathway. In addition, no up-regulation of Mad2, a critical SAC triggering protein [32, 33], was found during the mitotic arrest (Fig. 6C), suggesting SAC was not activated by the infection of ZD55SP/E1A-IL-24-shMPP1, and similar results were also observed in SW620 cells (data not shown).

We also found that compared with other rec-Ads, only the ZD55SP/E1A-IL-24-shMPP1 infection at low MOI induced senescence, a morphological change different from apoptosis or cytopathic effect. We used the SA-β-gal staining assay [34] to detect senescence in A549 cells induced by ZD55SP/E1A-IL-24-shMPP1. Senescence was observed at 0.5 MOI, but when the MOI was raised to 2 or higher, only apoptosis or cytopathic effect was detected (Fig. 6D), while no senescence was observed in other rec-Ads-treated cells (data not shown) suggest that even at low

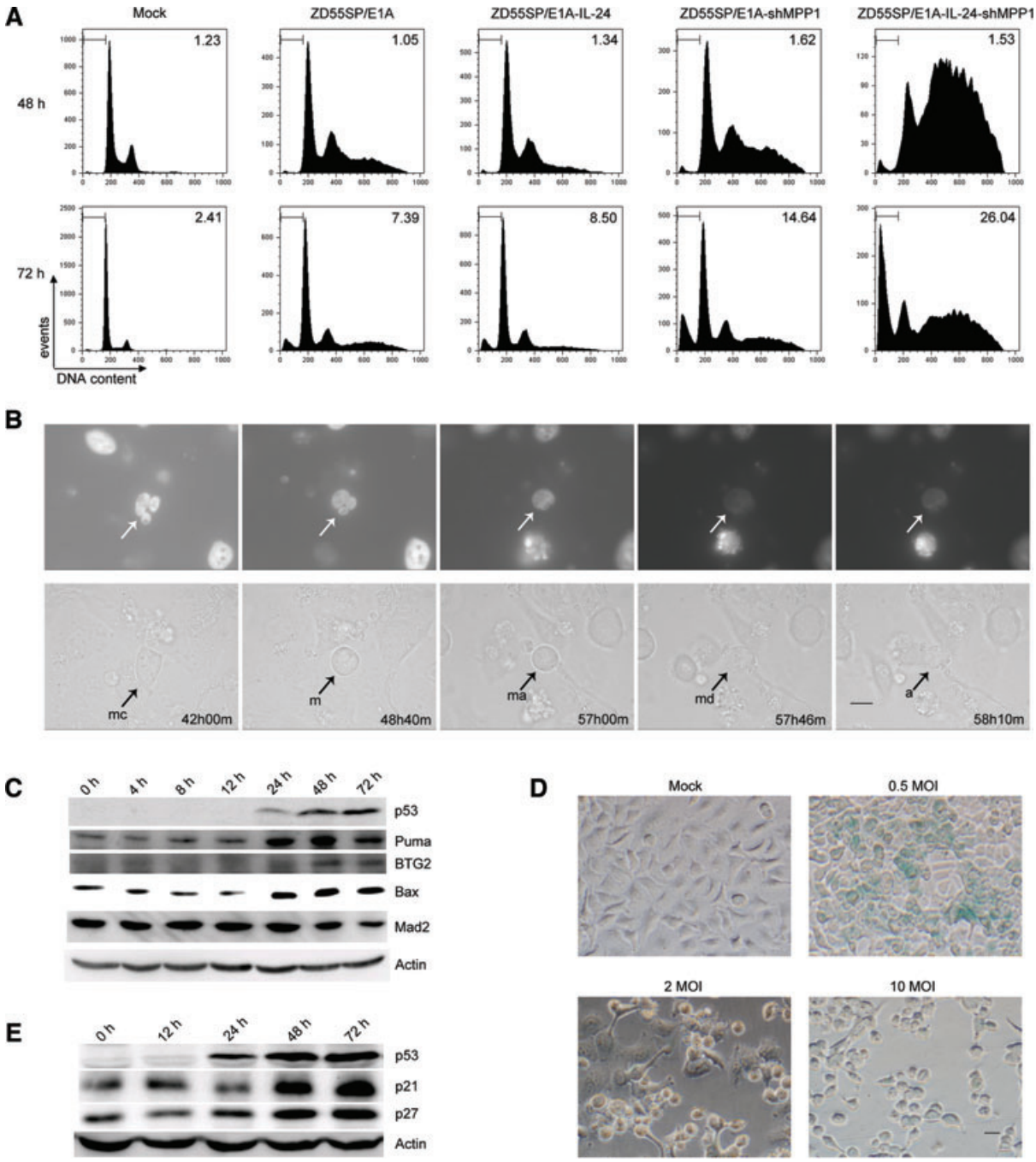

Fig. 6 ZD55SP/E1A-IL-24-shMPP1 induced mitotic arrest and senescence in tumour cells. (**A**) Apoptosis of A549 cells induced by infection was examined by FACS. The numbers show the percentage of cells in the sub-G_1 peak. (**B**) Selected frames of the time lapse phase-contrast microscopy videos show the cell cycle progression of the multinuclear A549 cells treated with ZD55SP/E1A-IL-24-shMPP1. Cells were transfected with plasmid H2B-RFP 4 hrs before the infection. The upper row, dark field, shows the cell nucleus; the lower row, bright field, shows the cell morphology. The arrows indicate the cells observed. Time is shown in hours and minutes. mc: multinuclear cell; m: mitosis; ma: mitotic arrest; md: mitotic defect; a: apoptosis. Scale bar: 20 μm. (**C**) The expression of p53 and its downstream genes and Mad2 protein in the process of mitotic arrest were studied by Western blot in A549 cells infected with ZD55SP/E1A-IL-24-shMPP1. (**A**–**C**) Cells were infected at MOI of 5. (**D**) Forty-eight hours after the infection with ZD55SP/E1A-IL-24-shMPP1 at different MOIs, A549 cells were visualized after SA-β-gal staining. The cells stained with blue indicate the SA-β-gal positive staining. Scale bar: 20 μm. (**E**) The expression of p53 and cell cycle suppressor genes were examined by Western blot in the senescence process of A549 cells induced by ZD55SP/E1A-IL-24-shMPP1 at MOI of 0.5.

MOI, ZD55SP/E1A-IL-24-shMPP1 could still inhibit tumour cells growth through triggering senescence. Western blot analysis revealed that p53 was also induced by the infection of ZD55SP/E1A-IL-24-shMPP1 at low MOI in A549 cells (Fig. 6E). The expression of cell cycle inhibition genes, p21 and p27, were up-regulated by infection as well, implying the cell cycle arrest caused by the infection of ZD55SP/E1A-IL-24-shMPP1 at low MOI, which thus further triggered senescence.

ZD55SP/E1A-IL-24-shMPP1 inhibits tumour growth *in vivo*

The *in vivo* oncolytic potential of ZD55SP/E1A-IL-24-shMPP1 was evaluated in a SW620 tumour xenografts model. As shown in Figure 7A, in PBS-treated group, the tumours grew rapidly and reached approximately 2100 mm^3 within 3 weeks, suggesting the high malignancy of the SW620 cells used in this study. However, the growth of ZD55SP/E1A-IL-24-shMPP1-treated tumours was obviously suppressed. Two months after treatment, the average volume of the ZD55SP/E1A-IL-24-shMPP1-treated tumours was 576 mm^3, significantly smaller than those with other rec-Ads treatments ($P < 0.001$; Fig. 7A) [21].

Immunohistochemistry was also used to evaluate the effect of the Ads on IL-24 and MPHOSPH1 expression *in vivo*. Seven days after treatment, the tumour specimens were separated from tumour-bearing mice. As shown in Fig. 7B, the MPHOSPH1 expression levels in the tumours treated with ZD55SP/E1A-IL-24-shMPP1 and ZD55SP/E1A-shMPP1 were markedly lower than those treated with PBS or ZD55SP/E1A; and IL-24 was also detected in tumours treated with ZD55SP/E1A-IL-24 and ZD55SP/E1A-IL-24-shMPP1. In all rec-Ads-treated tumours, the TUNEL analysis showed the cancer cells were undergoing apoptosis; in contrast, the PBS-treated tumour cells showed no signs of apoptosis. We thus deduced that ZD55SP/E1A-IL-24-shMPP1 may exert anti-tumour effect *in vivo* by combining the effects of up-regulation of IL-24, down-regulation of MPHOSPH1, and the oncolytic activity of the oncolytic vector, which subsequently induced apoptosis in tumour cells.

Discussion

Survivin has been reported as a cancer-specific up-regulated gene, and we had previously used its 1.1-kb promoter to construct a cancer targeted OV [26, 27]. To shorten its length and increase the capacity of OV in this study, we cloned a 269-bp survivin promoter inspired by the work of Xu *et al.* that identified this 269-bp protomer fragment has the strongest transcriptional activity within the full-length survivin promotor [25], and investigated its promoter properties. Our results revealed that the 269-bp survivin promoter had a remarkable tumour-selective transcriptional activity, and compared with the 1.1-kb promoter, the 269-bp promoter mediated much stronger reporter expression in tumour cells (data not shown). Because of its multiple advantages, for example, the small size, strict and strong tumour-specific transcriptional activity, the 269-bp survivin promoter is an ideal tumour selective target for cancer gene therapy.

We have previously reported that the CTGVT enhanced the anti-tumour effect of an oncolytic adenovirus by amplifying the tumour suppressor gene it carries during replication [17, 23, 35]. An appropriate tumour suppressor gene is critical for the success of the CTGVT, in this study, we investigated the anti-tumour effects of co-expression of two tumour suppressor genes, IL-24 and shMPP1, with our newly constructed ZD55SP/E1A vector. Our previous results that IL-24 an excellent candidate of anti-oncogene carried by oncolytic Ads [5, 6]. Another potential benefit of using IL-24 in this study is that the interferon effects, which can be induced by Ad infection and IL-24 treatment [36, 37], can up-regulate IL-24 and might further enhance anti-tumour effects of the oncolytic Ads [38, 39], and it will be of great interest to investigate this interferon effects in detail in the future. Compared to IL-24, MPHOSPH1 was only recently identified in bladder cancer as a novel oncogene [4]. Here, we demonstrated that MPHOSPH1 was up-regulated in many types of cancer cells, such as cells of liver cancer, lung cancer, colorectal cancer and ovarian cancer; moreover, we also targeted MPHOSPH1 for the first time in cancer gene therapy and achieved satisfying tumour suppression effects by inducing mitotic arrest and apoptosis of tumour cells.

Another interesting finding is that mitotic arrest induced by MPHOSPH1 knockdown did not up-regulate Mad2 that triggers SAC activation [32, 33], which is normally associated with the vinca alkaloids or taxanes treatment [1]. A possible explanation is that, rather than the neuron-microtubular perturbation side effect of alkaloids or taxanes treatment [2], MPHOSPH1 knockdown may exert effect on cytokinesis and trigger mitosis arrest without disturbing the cell spindle assembly. Thus, comparing with the traditional vinca alkaloids or taxanes treatment, MPHOSPH1 suppression may represent a better anti-mitotic cancer therapy strategy. However, more evidence is needed to test this hypothesis.

We also noted that although the MPHOSPH1 knockdown (by ZD55SP/E1A-shMPP1 infection) induced significant polyploidy in tumour cells, the further combination of IL-24 (ZD55SP/E1A-IL-24-shMPP1) significantly raised the anti-tumour activity (Fig. 6A). According to our Western blotting results, the ZD55SP/E1A-IL-24-shMPP1 was the only Ad resulted in the down-regulation of cIAP (Fig. 5F); therefore, IL-24 combined with shMPP1 may enhance anti-tumour effect by suppressing cIAP. It has been reported that cIAP can be induced upon virus infection [40, 41], we also found here that adenovirus infection induced cIAP expression; because cIAP is believed to protect the infected cells *via* blocking apoptosis [40, 41], thus it may explain the weak anti-tumour effects of OVs respectively harbouring IL-24 or shMPP1 alone. It will be of our future interests to study the relationship between IL-24 and MPHOSPH1. Our animal studies provide evidence that the combination of anti-mitotic MPHOSPH1 and IL-24 genes with CTGVT is a promising strategy for cancer gene therapeutics. Immunohistochemistry study showed that 30–50% of the tumour cells stained brown by anti-hexon antibody (data not shown),

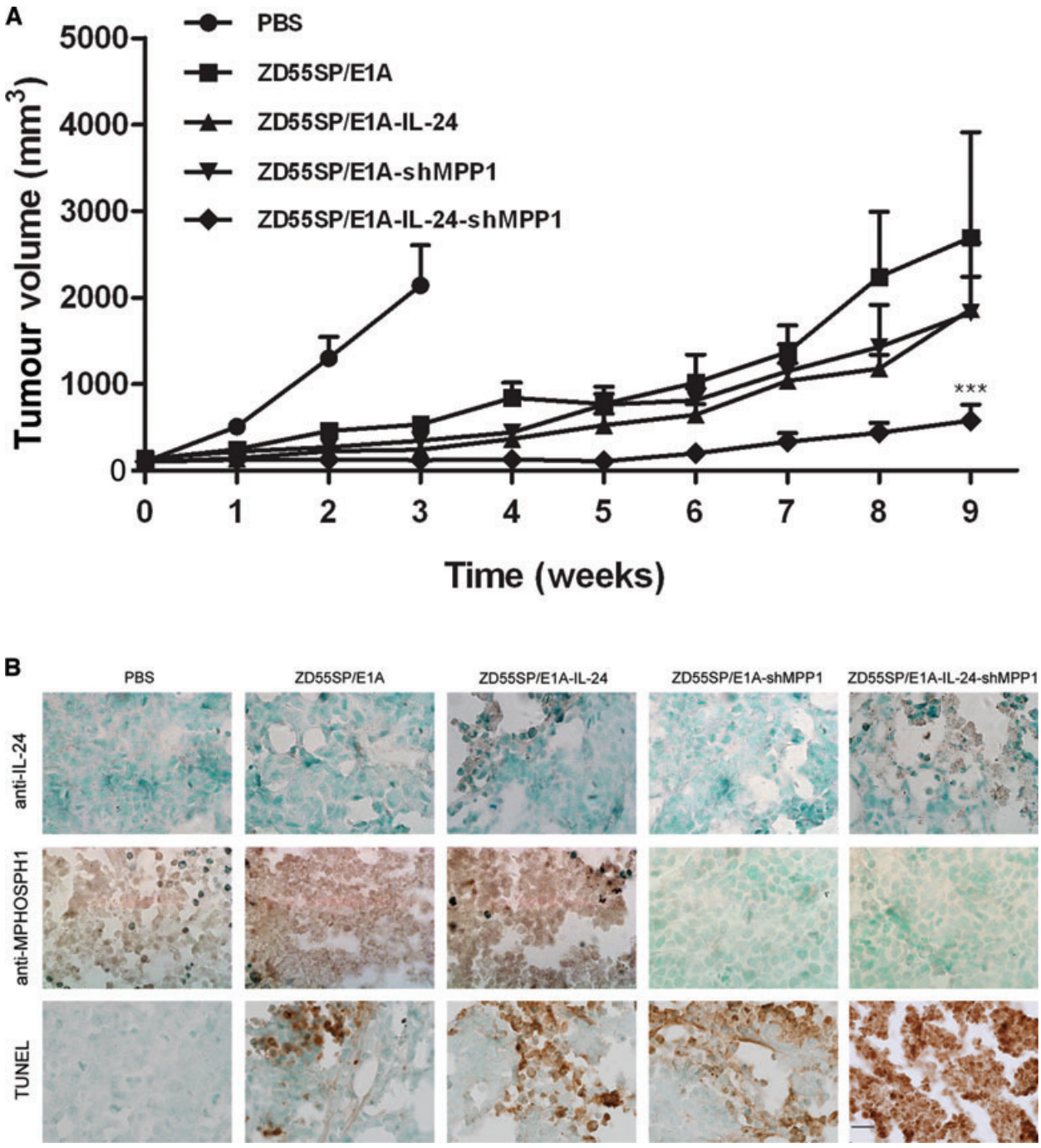

Fig. 7 ZD55SP/E1A-IL-24-shMPP1 inhibited the growth of the SW620 xenograft tumours. (**A**) Measurement of the tumour volume of different groups treated with oncolytic Ads or PBS every seven days. When tumours reached 100–150 mm^3 in volume, animals were injected with oncolytic Ads or PBS at week 0. Points indicate the mean values ($n = 7$); bars indicate S.D. ($^{***}P < 0.001$). (**B**) Immunostaining and TUNEL staining analysis of tumour sections derived from PBS or oncolytic Ads-treated tumours by IL-24 and MPHOSPH1. Scale bar: 20 μm.

which may be an index of infected cell number *in vivo*. Immunohistochemistry assay also indicated that three functions including viral oncolysis, IL-24 tumour suppression and MPHOSPH1 inhibition are involved in the apoptosis of tumour cells *in vivo* (Fig. 7B). Although the viral oncolysis and the single tumour suppressor gene expression both inhibit the xenograft tumours growth, the combined dual-construct nevertheless showed the highest anti-tumour ability *in vivo* (Fig. 7A).

Much work has been done to study the relationship between the cellular genome and cancer [42–45], however, it remains in debate whether the genome change of cell promotes or suppresses tumourigenesis. In this study, we found that the polyploidy induced by ZD55SP/E1A-IL-24-shMPP1 actually inhibited tumourigenesis through apoptosis. Because observed tumourigenesis suppression were obtained by oncolytic adenovirus infection, which can cause oncolytic effects by itself, it is thus possible that under other conditions, the cell genome change (aneuploidy or polyploidy) may be found to induce tumourigenesis. Our results may provide a new approach on this research.

Another interesting question raised regards how the infected cells with >4N DNA content came into being (Fig. 6A). A possible interpretation is that at anaphase or telophase, the cells with 4N DNA content may escape from the mitotic arrest induced by ZD55SP/E1A-IL-24-shMPP1 infection and exit mitosis without division (mitotic slippage), and subsequently initiate the next round of cell cycle and enter the S phase, at which their DNA is replicated (DNA content increased). Thus, the observed apoptosis of cells with >4N DNA may represent a type of post-mitotic apoptosis. We also found that p53, which promotes post-mitotic apoptosis due to its accumulation in the prolonged mitotic arrest [30], was involved in the apoptosis and senescence of the mitosis-arrested tumour cells induced by infection of ZD55SP/E1A-IL-24-shMPP1. Furthermore, it is interesting to note that infections of different MOI led to the different cellular changes (apoptosis or senescence) in this study. We believe a possible explanation is that the infection results depend on the initially infected cell number. When the initial percentage of infected cells is low, the infection might result in chronic effect such as senescence, whereas for high percentage of infected cells, acute effects such as CPE or apoptosis might be caused, although our results suggest that both low and high MOI infections will lead to more than 90% of the cells infected eventually (Fig. 3). However, further investigations are still in need.

Acknowledgements

We wish to thank Ying Xu, Tian Xiao, Lanying Sun, Jingfa Gu and Cell Analysis Center (Institute of Biochemistry and Cell Biology, Shanghai Institutes for Biological Sciences, Chinese Academy of Sciences) for professional technical assistance. We also appreciate the invaluable suggestions from two reviewers from the *Journal of Cellular and Molecular Medicine*, which greatly improve the quality of this paper. This work was supported by the National Basic Research Program of China (973 Program; No. 2010CB529901), Important National Science & Technology Specific Project of Hepatitis and Hepatoma Related Program (2008ZX10002-023), New Innovation Program (2009-ZX-09102-246), the Zhejiang Sci-Tech University grant (1016834-Y) and the Natural Science Foundation of China (Nos. 30801445 and 30970607).

Conflict of interest

The authors declare no conflict of interest.

Supporting Information

Additional Supporting Information may be found in the online version of this article.

Fig. S1 RNA interference effects of four constructed plasmids expressing shMPP1 were valued by RT-PCR.

Fig. S2 Identification of the rec-Ads.

Please note: Wiley-Blackwell is not responsible for the content or functionality of any supporting materials supplied by the authors. Any queries (other than missing material) should be directed to the corresponding author for the article.

References

1. **McGrogan BT, Gilmartin B, Carney DN, *et al.*** Taxanes, microtubules and chemoresistant breast cancer. *Biochim Biophys Acta.* 2008; 1785: 96–132.
2. **Jordan MA, Wilson L**. Microtubules as a target for anticancer drugs. *Nat Rev Cancer.* 2004; 4: 253–65.
3. **Abaza A, Soleilhac JM, Westendorf J, *et al.*** M phase phosphoprotein 1 is a human plus-end-directed kinesin-related protein required for cytokinesis. *J Biol Chem.* 2003; 278: 27844–52.
4. **Kanehira M, Katagiri T, Shimo A, *et al.*** Oncogenic role of MPHOSPH1, a cancer-testis antigen specific to human bladder cancer. *Cancer Res.* 2007; 67: 3276–85.
5. **Zhao L, Gu J, Dong A, *et al.*** Potent antitumour activity of oncolytic adenovirus expressing mda-7/IL-24 for colorectal cancer. *Hum Gene Ther.* 2005; 16: 845–58.
6. **Zhao L, Dong A, Gu J, *et al.*** The antitumour activity of TRAIL and IL-24 with replicating oncolytic adenovirus in colorectal cancer. *Cancer Gene Ther.* 2006; 13: 1011–22.
7. **Lebedeva IV, Sarkar D, Su ZZ, *et al.*** Bcl-2 and Bcl-x(L) differentially protect human prostate cancer cells from induction of apoptosis by melanoma differentiation associated gene-7, mda-7/IL-24. *Oncogene.* 2003; 22: 8758–73.

8. **Lebedeva IV, Su ZZ, Sarkar D, *et al.*** Melanoma differentiation associated gene-7, mda-7/interleukin-24, induces apoptosis in prostate cancer cells by promoting mitochondrial dysfunction and inducing reactive oxygen species. *Cancer Res.* 2003; 63: 8138–44.
9. **Yacoub A, Gupta P, Park MA, *et al.*** Regulation of GST-MDA-7 toxicity in human glioblastoma cells by ERBB1, ERK1/2, PI3K, and JNK1–3 pathway signaling. *Mol Cancer Ther.* 2008; 7: 314–29.
10. **Yacoub A, Hamed H, Emdad L, *et al.*** MDA-7/IL-24 plus radiation enhance survival in animals with intracranial primary human GBM tumours. *Cancer Biol Ther.* 2008; 7: 917–33.
11. **Yacoub A, Hamed HA, Allegood J, *et al.*** PERK-dependent regulation of ceramide synthase 6 and thioredoxin play a key role in mda-7/IL-24-induced killing of primary human glioblastoma multiforme cells. *Cancer Res.* 2010; 70: 1120–9.
12. **Yacoub A, Liu R, Park MA, *et al.*** Cisplatin enhances protein kinase R-like endoplasmic reticulum kinase- and CD95-dependent melanoma differentiation-associated gene-7/interleukin-24-induced killing in ovarian carcinoma cells. *Mol Pharmacol.* 2009; 77: 298–310.
13. **Bhutia SK, Dash R, Das SK, *et al.*** Mechanism of autophagy to apoptosis switch triggered in prostate cancer cells by antitumour cytokine melanoma differentiation-associated gene 7/interleukin-24. *Cancer Res.* 2010; 70: 3667–76.
14. **Yacoub A, Mitchell C, Lister A, *et al.*** Melanoma differentiation-associated 7 (interleukin 24) inhibits growth and enhances radiosensitivity of glioma cells *in vitro* and *in vivo*. *Clin Cancer Res.* 2003; 9: 3272–81.
15. **Kreis S, Philippidou D, Margue C, *et al.*** IL-24: a classic cytokine and/or a potential cure for cancer? *J Cell Mol Med.* 2008; 12: 2505–10.
16. **Liu X.** A new antitumour strategy: cancer gene-viro-therapy. *Chin J Cancer Biother.* 2001; 8: 1–2.
17. **Zhang ZL, Zou WG, Luo CX, *et al.*** An armed oncolytic adenovirus system, ZD55-gene, demonstrating potent antitumoral efficacy. *Cell Res.* 2003; 13: 481–9.
18. **Bischoff JR, Kirn DH, Williams A, *et al.*** An adenovirus mutant that replicates selectively in p53-deficient human tumour cells. *Science.* 1996; 274: 373–6.
19. **Heise C, Sampson-Johannes A, Williams A, *et al.*** ONYX-015, an E1B gene-attenuated adenovirus, causes tumour-specific cytolysis and antitumoral efficacy that can be augmented by standard chemotherapeutic agents. *Nat Med.* 1997; 3: 639–45.
20. **Chu L, Gu J, Sun L, *et al.*** Oncolytic adenovirus-mediated shRNA against Apollon inhibits tumour cell growth and enhances antitumour effect of 5-fluorouracil. *Gene Ther.* 2008; 15: 484–94.
21. **Xiao T, Fan JK, Huang HL, *et al.*** VEGI-armed oncolytic adenovirus inhibits tumour neovascularization and directly induces mitochondria-mediated cancer cell apoptosis. *Cell Res.* 2010; 20: 367–78.
22. **Wei N, Fan JK, Gu JF, *et al.*** A double-regulated oncolytic adenovirus with improved safety for adenocarcinoma therapy. *Biochem Biophys Res Commun.* 2009; 388: 234–9.
23. **Zou W, Luo C, Zhang Z, *et al.*** A novel oncolytic adenovirus targeting to telomerase activity in tumour cells with potent. *Oncogene.* 2004; 23: 457–64.
24. **Li F, Altieri DC**. Transcriptional analysis of human survivin gene expression. *Biochem J.* 1999; 344: 305–11.
25. **Bao R, Connolly DC, Murphy M, *et al.*** Activation of cancer-specific gene expression by the survivin promoter. *J Natl Cancer Inst.* 2002; 94: 522–8.
26. **Xu R, Zhang P, Huang J, *et al.*** Sp1 and Sp3 regulate basal transcription of the survivin gene. *Biochem Biophys Res Commun.* 2007; 356: 286–92.
27. **Li B, Liu X, Fan J, *et al.*** A survivin-mediated oncolytic adenovirus induces non-apoptotic cell death in lung cancer cells and shows antitumoral potential *in vivo*. *J Gene Med.* 2006; 8: 1232–42.
28. **Jonsson G, Paulie S, Grandien A.** cIAP-2 block apoptotic events in bladder cancer cells. *Anticancer Res.* 2003; 23: 3311–6.
29. **Tanimoto T, Tsuda H, Imazeki N, *et al.*** Nuclear expression of cIAP-1, an apoptosis inhibiting protein, predicts lymph node metastasis and poor patient prognosis in head and neck squamous cell carcinomas. *Cancer Lett.* 2005; 224: 141–51.
30. **Blagosklonny MV.** Mitotic arrest and cell fate: why and how mitotic inhibition of transcription drives mutually exclusive events. *Cell Cycle.* 2007; 6: 70–4.
31. **Zhang L, Zhang J, Hu C, *et al.*** Efficient activation of p53 pathway in A549 cells exposed to L2, a novel compound targeting p53-MDM2 interaction. *Anticancer Drugs.* 2009; 20: 416–24.
32. **Niault T, Hached K, Sotillo R, *et al.*** Changing Mad2 levels affects chromosome segregation and spindle assembly checkpoint control in female mouse meiosis I. *PLoS One.* 2007; 2: e1165.
33. **De Antoni A, Pearson CG, Cimini D, *et al.*** The Mad1/Mad2 complex as a template for Mad2 activation in the spindle assembly checkpoint. *Curr Biol.* 2005; 15: 214–25.
34. **Tao Q, Lv B, Qiao B, *et al.*** Immortalization of ameloblastoma cells *via* reactivation of telomerase function: phenotypic and molecular characteristics. *Oral Oncol.* 2009; 45: e239–44.
35. **Cao X, Yang M, Wei RC, *et al.*** Cancer targeting Gene-Viro-Therapy of liver carcinoma by dual-regulated oncolytic adenovirus armed with TRAIL gene. *Gene Ther.* 2011; 18: 765–77.
36. **Feigenblum D, Walker R, Schneider RJ**. Adenovirus induction of an interferon-regulatory factor during entry into the late phase of infection. *J Virol.* 1998; 72: 9257–66.
37. **Ekmekcioglu S, Mumm JB, Udtha M, *et al.*** Killing of human melanoma cells induced by activation of class I interferon-regulated signaling pathways *via* MDA-7/IL-24. *Cytokine.* 2008; 43: 34–44.
38. **Oritani K, Kanakura Y.** IFN-zeta/limitin: a member of type I IFN with mild lymphomyelosuppression. *J Cell Mol Med.* 2005; 9: 244–54.
39. **Jiang H, Lin JJ, Su ZZ, *et al.*** Subtraction hybridization identifies a novel melanoma differentiation associated gene, mda-7, modulated during human melanoma differentiation, growth and progression. *Oncogene.* 1995; 11: 2477–86.
40. **James MA, Lee JH, Klingelhutz AJ.** Human papillomavirus type 16 E6 activates NF-kappaB, induces cIAP-2 expression, and protects against apoptosis in a PDZ binding motif-dependent manner. *J Virol.* 2006; 80: 5301–7.
41. **Zane L, Sibon D, Legras C, *et al.*** Clonal expansion of HTLV-1 positive CD8+ cells relies on cIAP-2 but not on c-FLIP expression. *Virology.* 2010; 407: 341–51.
42. **Sotillo R, Hernando E, Diaz-Rodriguez E, *et al.*** Mad2 overexpression promotes aneuploidy and tumorigenesis in mice. *Cancer Cell.* 2007; 11: 9–23.
43. **Pellman D.** Cell biology: aneuploidy and cancer. *Nature.* 2007; 446: 38–9.
44. **Weaver BA, Silk AD, Montagna C, *et al.*** Aneuploidy acts both oncogenically and as a tumour suppressor. *Cancer Cell.* 2007; 11: 25–36.
45. **Hernando E, Nahle Z, Juan G, *et al.*** Rb inactivation promotes genomic instability by uncoupling cell cycle progression from mitotic control. *Nature.* 2004; 430: 797–802.